The American Journal of Cardiology 266 (2026) 59–66

Contents lists available at ScienceDirect

The American Journal of Cardiology

journal homepage: www.elsevier.com/locate/ajc

Estimated Stressed Blood Volume in Patients With Cardiac Amyloidosis

Simon Vanhentenrijk, MD, PharmD[a], Silvio Nunes Augusto JrBSc[b,g], Pieter Martens, MD, PhD[c], Lauren Ives, RN[a], Sanjeeb Bhattacharya, MD[a,d], Andres Carmona-Rubio, MD[a], J. Emanuel Finet, MD[a,d], Miriam Jacob, MD[a,d], Trejeeve Martyn, MD, MSc[a,d], Jason Valent, MD[d,e], Mazen Hanna, MD[a,d], Daniel Burkhoff, MD, PhD[f], Wai Hong Wilson Tang, MD[a,b,d*]

[a] *Kaufman Center for Heart Failure Treatment and Recovery, Heart Vascular and Thoracic Institute, Cleveland Clinic, Cleveland, Ohio*
[b] *Department of Cardiovascular and Metabolic Sciences, Lerner Research Institute, Cleveland Clinic, Cleveland, Ohio*
[c] *Department of Cardiology, Ziekenhuis Oost-Limburg, Genk, and the Faculty of Medicine and Life Sciences, Hasselt University, Hasselt, Belgium*
[d] *Cleveland Clinic Lerner College of Medicine of Case Western Reserve University, Cleveland, Ohio*
[e] *Department of Hematology and Medical Oncology, Taussig Cancer Institute, Cleveland Clinic, Cleveland, Ohio*
[f] *Cardiovascular Research Foundation, New York, New York*
[g] *MetroHealth System, Cleveland, Ohio*

ARTICLE INFO

Article History:
Received 27 November 2025
Revised 13 January 2026
Accepted 10 February 2026

Keywords:
stressed blood volume
cardiac amyloidosis
hemodynamics
clinical outcomes

Hemodynamic profiles in cardiac amyloidosis (CA) patients differ from traditional heart failure phenotypes. Stressed blood volume is a main determinant of intravascular pressures and affect cardiac filling pressures. We hypothesized that estimated stressed blood volume (eSBV) may help us better understand hemodynamic derangements in patients with CA and its relation to adverse outcomes. We reviewed 462 consecutive patients who underwent right heart catheterization at a tertiary care institution for eSBV based on basic hemodynamic measurements. Median eSBV was used to stratify for high versus low eSBV. The primary outcome was all-cause mortality of high versus low eSBV in CA patients with left ventricular ejection fraction (LVEF) >40% or LVEF ≤ 40%. In our final cohort of 388 patients, of which 225 (58%) had transthyretin CA and 163 (42%) had light-chain CA, the median eSBV was 2,191 ml/70 kg. Among those with LVEF > 40%, 42 (16.6%) patients with high eSBV, while 27 (10.7%) patients with low eSBV developed adverse events (log-rank p = 0.018). Higher eSBV was independently associated with a higher risk of all-cause mortality (HR 1.84, 95% cardiac index 1.12 to 3.01, p = 0.015) even after adjustments for traditional cardiovascular risk factors, LVEF, and NT-proBNP (HR 2.19, 95% cardiac index 1.19 to 4.03, p = 0.012). Conversely, high eSBV did not predicted poor outcome in the LVEF ≤ 40% cohort. In conclusion, eSBV is an independent predictor of all-cause mortality in patients with CA and LVEF > 40% even after adjustment for traditional cardiovascular risk factors. Modelling eSBV through integrating established invasive hemodynamic parameters may become a valuable asset in the contemporary heart failure unit to guide treatment decision-making and prognosis.

Cardiac amyloidosis (CA) is caused by progressive infiltration of amorphous, fibrillar proteinaceous material in the myocardial extracellular space, leading to a restrictive cardiomyopathy phenotype.[1,2] Transthyretin (TTR), light-chain (AL), or non-TTR/AL amyloidogenic precipitants accumulate throughout the myocardial extracellular space and vasculature, which alters normal physiologic hemodynamics. Over time, this results in stiffer atria and ventricles and a less compliant arterial and venous capacitance systems, the latter predominantly featuring in AL-CA.

Invasive hemodynamic profiling of various heart failure (HF) phenotypes was first described in 1976 by Forrester and Diamond.[3] Although CA hemodynamics are largely underrepresented in HF trials, hemodynamic alterations and their prognostic value in CA patients have recently been reconsidered.[4] Also, the degree of amyloid infiltration directly determines the severity of the restrictive phenotype, which is reflected by the hemodynamic profile. Hence, the hemodynamic phenotype should correlate with outcomes, since the degree of infiltration correlates with outcomes.[5] Furthermore, the majority of CA patients (irrespective of CA subtype) features elevated left- and right-sided cardiac filling pressures at rest, which advocates using higher hemodynamic cutoffs compared with patients with nonamyloid HF to predict clinical outcome.[4]

Abbreviations: AL, light-chain; CA, cardiac amyloidosis; eSBV, estimated stressed blood volume; HF, heart failure; LVEF, left ventricular ejection fraction; TTR, transthyretin

Funding: None.

*Corresponding author: Tel: (216) 444-2121; fax: (216) 445-6165.
E-mail address: tangw@ccf.org (W.H.W. Tang).

https://doi.org/10.1016/j.amjcard.2026.02.025

The total blood volume (TBV) of the circulatory system can be divided, functionally, into unstressed and stressed blood components.[6] Stressed blood volume (not TBV) is a main determinant of intravascular pressures.[6] Alternations of TBV and venous tone (either through venoconstriction or venodilation) affect stressed blood volume, which accordingly, further determine cardiac filling pressures. Given the aforementioned myocardial and vascular repercussions of longstanding amyloid deposition, venous compliance and capacitance may be reduced, which along with increased sympathetic tone present in all forms of HF, may lead to alternations of the stressed blood volume portion TBV in patients with CA. As we hypothesized that estimated stressed blood volume (eSBV) may help us better understand hemodynamic derangements in patients with CA, the goals of our analysis were[1]: to describe eSBV in CA patients and its correlation with traditional hemodynamic parameters[2]; to assess how eSBV in CA patients relate to clinical outcomes.

Methods

Study population

Consecutive patients diagnosed with CA at a tertiary care institution between January 2001 and August 2021 were screened for participation. Patient characteristics have been previously described by Martens et al,[4] whereas the median duration between right heart catheterization (RHC) and diagnosis of CA was 0 days (−8 to 0 days). The diagnosis of TTR CA (ATTR-CA) was either established from routine tissue biopsy or a standardized noninvasive assessment in both the outpatient and inpatient cohort.[4] The indication for RHC were in descending order of frequency: part of a procedure with concomitant endomyocardial biopsy (EMB), RHC for acute on chronic HF with need for invasive hemodynamic monitoring, part of an evaluation for pulmonary hypertension, part of an evaluation for idiopathic cardiomyopathy/dyspnea (without EMB), as part of an evaluation of bridging to advanced therapies (eg, LVAD or heart transplant), and as an evaluation of progressive cardio-renal syndrome. When an EMB was performed, confirmation of TTR deposition in tissue specimen was found by either immunogold electron microscopy, immunohistochemistry, or mass spectrometry. Alternatively, noninvasive diagnosis of ATTR-CA was established through all the following[1]: signs and symptoms of HF supported with an echocardiogram or cardiac magnetic resonance imaging consistent with or suggestive of CA[2]; grade 2 or 3 cardiac uptake on a technetium pyrophosphate scan confirmed by single-photon emission computerized tomography/computerized tomography; and[3] absence of a detectable monoclonal protein on serum or urine immunofixation electrophoresis or serum free light chain assay.[7] The diagnosis of AL-CA was established through multimodality imaging (eg, echocardiography or cardiac magnetic resonance imaging) supported with abnormal serum or urine immunofixation electrophoresis or abnormal serum free light chain assay, with ultimate confirmation based on the presence of light chain amyloid deposits on biopsy (either cardiac or extracardiac biopsy).

Data synthesis

Patient demographics, comorbidities, medical history, laboratory features, medical therapies, electrocardiogram, echocardiogram, pressures, and cardiac output from RHC and technetium pyrophosphate scans were all retrieved from the prospectively maintained REDCap database. Patients were stratified based on EF.

Outcomes

The primary outcome was all-cause mortality, comparing patients with high versus low eSBV in CA patients with left ventricular ejection fraction (LVEF) >40% or LVEF ≤ 40%. Uni- and multivariable analysis for the primary endpoint of all-cause mortality where enclosed in the survival analysis.

Hemodynamic measurements and definitions

RHC was performed according to institutional standards, at baseline in the catheterization laboratory at rest and in the supine position. A balloon-tipped, fluid-filled catheter was used to obtain mean right atrial pressure (RAP), right ventricular pressures, pulmonary artery systolic and diastolic pressures, as well as pulmonary capillary wedge pressure (PCWP). All measurements were obtained at end expiration under steady state conditions. PCWP was measured at the end of expiration after a spontaneous breathing cycle. Cardiac output was measured using thermodilution, and cardiac index (CI) was calculated as cardiac output divided by body surface area. Stroke volume index (SVi) was derived from CI using instantaneous heart rate. Systolic and diastolic blood pressures were obtained using a digital sphygmomanometer at the time of the procedure.

Estimation of stressed blood volume

TBV is functionally divided into UBV and SBV pools: TBV = UBV + SBV. Direct measurement of UBV and SBV necessitates thorough experimental maneuvers, which are not readily applicable to humans. As such, we applied a simulation-based method for estimating SBV based on widely used models of the cardiovascular system.[8] In brief, the systemic and pulmonary circulations are represented by series of resistors and capacitors, whereas the cardiac chambers are featured by individual time-varying elastances.[9–13] The nonlinear, time-varying differential equations governing this model can be solved by numeric integration. For estimation of the SBV, the measured values of heart rate, cardiac output, RAP, PCWP, systolic PAP, diastolic PAP, systolic and diastolic aortic pressures, and LVEF for a given patient and condition were provided to the model. The algorithm unbiasedly searches the multidimensional space composed of the model parameters to optimize the agreement of all hemodynamic parameter measurements with the model output. The algorithm is implemented in the real-time simulation (retrieved online from http://harvi.online, Harvi Dynamics Inc). Aside from heart rate, each of the other 8 variables represents a measured parameter that must be matched by the output of the model on a patient-by-patient basis. Model parameter values that are optimized include RV and left ventricular end-systolic elastances and diastolic stiffness constants, systemic and PA compliances and characteristic impedances, and, finally, eSBV. To account for differences in patient sizes, all eSBV values are presented as milliliters per 70 kg body weight. TBV was estimated using body weight, as described previously[14] (detailed description of SBV measurement is provided in the Supplementary Materials). Unstressed blood volume was calculated as the difference of TBV and eSBV.

Statistical analysis

Continuous variables are summarized as mean ± standard deviation if normally distributed and median (interquartile range) if not normally distributed. Chi-square analysis was used to compare categorical variables. Mann–Whitney *U* test was used for continuous variables as appropriate. Spearman analysis was performed to assess nonparametric correlations between eSBV and other hemodynamic

parameters. Ordinal regression was used to determine relation between functional status and hemodynamic variables, with the reporting of a standardized estimate (*Z* scores) to allow unitless strength comparison between hemodynamic variables using different units and thus measurement scale. Survival analysis was established by Kaplan–Meier analysis and univariable and multivariable Cox proportional hazard models for primary outcome. Multivariable survival models included adjustments for covariates such as age, sex, hypertension, body mass index, LVEF, and NT-proBNP. All analyses were performed with R (RStudio 2024.09.1 + 394) and SPSS (SPSS, Chicago, IL, version 29.0.2.0), and a two-sided p value <0.05 was considered statistically significant.

Data availability

The data, analytic methods, and study materials will not be made available to other researchers for purposes of reproducing the results or replicating the procedures. There are restrictions related to the availability of some of the clinical data generated in the present study because we do not have permission in our informed consent from research subjects to share data outside our institution without their authorizations. The authors had full access to all the data in the study and take responsibility for the integrity of the data and accuracy of the data analysis, and may agree to make aggregate data available upon reasonable request.

This study has been approved by our Institutional Review Board, and written informed consent was waived as all procedures were performed as part of the routine clinical care. The manuscript was designed according to the Strengthening the Reporting of Observational Studies in Epidemiology statement for observational studies.[15]

Results

Patient population

Between January 2001 and August 2021, a total of 1,556 patients received a diagnosis of CA, of whom 466 underwent RHC at baseline (33%). For this analysis, we included 388 patients. Figure 1 outlines a STROBE diagram illustrating the patient flow throughout the study. Table 1 provides the baseline characteristics of patients with CA stratified by high versus low eSBV. Cohorts for high and low eSBV were created based on the median eSBV of the total cohort. There were no significant differences in baseline characteristics between patients with high eSBV compared with low eSBV. Patients with low eSBV were more likely to receive beta-blocker therapy (59%). Yet, nearly half of the cohort featured prior diagnosis of atrial fibrillation. Only one in five patients did not receive maintenance diuretic therapy. Subsequently, distinctive cohorts were defined based on EF strata. Both LVEF > 40% and LVEF ≤ 40% cohorts featured different phenotypical background as outlined in Supplemental Tables 1 and 2.

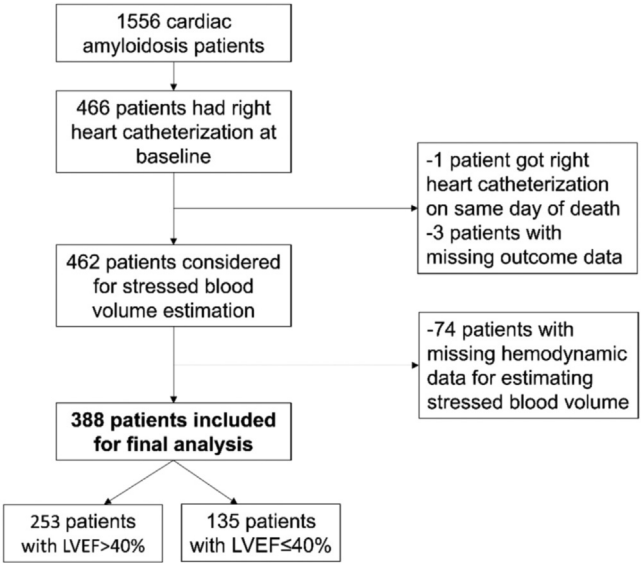

Figure 1. STROBE diagram displaying patient selection for different phases of the study.

Baseline hemodynamics

Table 1 compares cardiovascular hemodynamics between cohorts with high versus low eSBV. Overall, patients featured a warm- and wet-hemodynamic phenotype with markedly elevated biventricular filling pressures and preserved cardiac output. Median eSBV was not significantly different between AL-CA and ATTR-CA patients. In the LVEF ≤ 40% cohort, patients with elevated eSBV were more likely to feature high right-sided filling pressures compared with patients with low eSBV. Also, left ventricular end-systolic elastance (LV E_{es}), an established marker to quantify LV contractility, was similarly provided as an output of the HARVI model, appeared to be significantly lower in the high eSBV compared with the low eSBV cohort. Patients with higher eSBV showed slightly (not statistically significant) lower systemic vascular resistance and higher pulmonary vascular resistance.

Determinants of eSBV in patients with CA

A binary regression model was implemented to determine hemodynamic predictors of high eSBV for both EF strata (Supplemental Table 3). In the LVEF > 40% cohort, the majority of variables showing predictive capacity of high eSBV were markers of right-sided congestion. As such, elevated RAP, PASP, PADP, mPAP demonstrate strong predictive values for high eSBV (Figure 2). PCWP was the only left-sided hemodynamic marker of predicting high eSBV. Also, the RAP/PCWP ratio and right ventricular cardiac power output both strongly correlated with elevated eSBV. Moreover, in CA patients with LVEF ≤ 40%, no single hemodynamic variable was capable of predicting elevated eSBV (Figure 2). Subsequently, we calculated the correlation of eSBV to established hemodynamic parameters in the LVEF > 40% cohort. In fact, estimated eSBV weakly correlated with RAP ($r = 0.213$; $p = 0.001$), PCWP ($r = 0.141$; $p = 0.028$) and RAP/PCWP ratio ($r = 0.137$; $p = 0.033$) (Supplemental Table 4). eSBV was inversely correlated with LV E_{es} ($r = -0.165$; $p = 0.009$) (Supplemental Table 4). Additionally, using receiver-operating curves, we observed that RAP (0.643, $p < 0.001$), mPAP (0.630, $p = 0.001$), right ventricular cardiac power output (0.607, $p = 0.008$), and not CO/70 kg (0.516, $p = 709$) predicted high eSBV in the LVEF > 40% cohort (figures not shown). In addition, receiver-operating curves with the Youden Index were also employed to determine an optimal eSBV threshold for predicting adverse outcomes. However, since no robust cut-off was found (Youden Index < 0.5), this analysis was discontinued.

SBV in relation to survival

During a follow-up period of 365 days, a total of 68 events occurred, of which 25 (19.7%) occurred in the low eSBV group, and 43 (34%) occurred in the high eSBV group for patients with LVEF > 40%. Unadjusted Kaplan–Meier curves for high and low eSBV are presented for the primary end-point of all-cause mortality in the LVEF > 40% cohort (Figure 3) and the LVEF ≤ 40% cohort (Figure 3). In LVEF > 40% patients, higher eSBV was independently associated with a higher risk of all-cause mortality (HR 1.84, 95% CI 1.12 to 3.01, p = 0.015). Similarly, after adjustment for traditional cardiovascular risk factors age, sex, smoking, body mass index, LVEF, and NT-

Table 1
Baseline characteristics stratified by low and high eSBV in the total cohort

Parameters	Total (*N* = 388)	Low eSBV/70 kg (*N* = 195)	High eSBV/70 kg (*N* = 193)	p value
Demographics				
Age, years	71 ± 10	70 ± 10	72 ± 10	0.576
Male	297 (77%)	151 (77%)	146 (76%)	0.138
Ethnicity				
Black	81 (21%)	40 (21%)	41 (21%)	0.844
White	295 (76%)	148 (76%)	147 (76%)	0.844
Other	12 (3%)	7 (4%)	5 (3%)	0.844
History of smoking	210 (54%)	104 (54%)	106 (56%)	0.154
Type of cardiac amyloidosis				
ATTR-CA	225 (58%)	118 (60%)	107 (54%)	0.237
AL-CA	163 (42%)	77 (40%)	86 (46%)	0.237
Comorbidities				
Hypertension	247 (64%)	117 (60%)	130 (67%)	0.693
Dyslipidemia	240 (62%)	119 (61%)	121 (63%)	0.104
Diabetes	102 (26%)	48 (25%)	54 (28%)	0.318
CAD	182 (47%)	93 (48%)	89 (50%)	0.132
Stroke	46 (12%)	26 (13%)	20 (10%)	0.305
Atrial fibrillation	209 (54%)	106 (55%)	103 (53%)	0.176
Pacemaker	104 (27%)	59 (30%)	45 (23%)	0.533
ICD	53 (14%)	33 (17%)	20 (11%)	0.616
BMI > 30 (kg/m^2)	98 (26%)	53 (28%)	45 (24%)	0.195
Weight, kg	79 ± 18	79 ± 18	79 ± 18	0.584
Heart failure measurements				
NYHA class				0.465
I	11 (3%)	3 (2%)	8 (5%)	
II	114 (32%)	57 (32%)	57 (32%)	
III	208 (59%)	108 (60%)	100 (57%)	
IV	22 (6%)	11 (6%)	11 (6%)	
cTnI (ng/ml)	0.10 ± 0.14	0.106 ± 0.12	0.10 ± 0.16	0.615
NT-proBNP (ng/ml)	7,471 ± 10,791	8,172 ± 12,178	6,812 ± 9,293	0.293
Medications				
MRA	101 (26%)	46 (24%)	55 (28%)	0.458
Diuretic	320 (83%)	158 (81%)	162 (84%)	0.288
Digoxin	46 (12%)	24 (12%)	22 (11%)	0.096
ACE/ARB	149 (39%)	79 (41%)	70 (37%)	0.400
Beta-blocker	137 (54%)	115 (59%)	97 (50%)	0.887
CCB	35 (9%)	15 (8%)	20 (11%)	0.274
Echocardiographic measurements				
LVEF, %	46 ± 14	47 ± 14	46 ± 13	0.389
LAVi, ml/m^2	48 ± 23	47 ± 25	49 ± 21	0.368
LVEDV, ml	93 ± 35	90 ± 31	96 ± 39	0.276
LVESV, ml	50 ± 25	46 ± 20	54 ± 28	0.170
GLS, %	−9.3 ± 3.7	−9.2 ± 3.7	−9.4 ± 3.7	0.336
Hemodynamic measurements				
eSBV, ml/70 kg	2,191 ± 2,660	1,753 ± 1,227	2,575 ± 1,431	**<0.001**
eUBV, ml	2,548 ± 962	3,075 ± 5,755	2,082 ± 5,134	**<0.001**
eTBV, ml	4,692 ± 5,517	4,733 ± 5,387	4,669 ± 4,717	0.493
HR, bpm	79 ± 15	79 ± 15	79 ± 15	0.954
Systolic BP, mm Hg	119 ± 21	118 ± 21	120 ± 21	0.255
Diastolic BP, mm Hg	75 ± 13	73 ± 12	76 ± 13	0.072
RAP, mm Hg	12 ± 6	11 ± 5	13 ± 6	**<0.001**
PASP, mm Hg	48 ± 15	46 ± 15	50 ± 14	**0.023**
PADP, mm Hg	23 ± 7	21 ± 7	24 ± 7	**0.023**
mPAP, mm Hg	30 ± 10	29 ± 10	32 ± 10	**0.001**
PCWP, mm Hg	21 ± 7	20 ± 7	22 ± 7	**0.007**
PVR, WU	2.9 ± 5.7	2.5 ± 1.5	3.3 ± 7.9	0.927
SVR, mm Hg/min per ml	1,524 ± 540	1,523 ± 495	1,526 ± 582	0.698
DPG, mm Hg	1.9 ± 6.1	1.5 ± 5.7	2.3 ± 6.6	0.896
TPG, mm Hg	11.9 ± 19.8	10.3 ± 5.7	13.4 ± 27.5	0.718
RAP/PCWP ratio	0.56 ± 0.25	0.53 ± 0.26	0.57 ± 0.25	0.175
API	2.39 ± 1.89	2.57 ± 2.20	2.21 ± 1.31	0.289
PAPi	2.8 ± 2.2	2.9 ± 2.4	2.6 ± 1.9	0.100
LVCPO, Watt	0.90 ± 0.37	0.87 ± 0.35	0.92 ± 0.40	0.713
RVCPO, Watt	0.31 ± 0.14	0.29 ± 0.12	0.33 ± 0.15	0.091
PAC, ml/mm Hg	2.4 ± 2.0	2.2 ± 1.7	2.5 ± 2.2	0.178
SAC, ml/mm Hg	1.6 ± 4.7	1.8 ± 6.4	1.3 ± 0.8	0.421
CO/70 kg, L/min	4.5 ± 1.7	4.4 ± 1.4	4.6 ± 1.9	0.996
CI/70 kg, L/min/m^2	2.2 ± 0.6	2.2 ± 0.6	2.2 ± 0.6	0.833
PP (mm Hg)	44 ± 15	45 ± 16	44 ± 15	0.969

(*continued*)

Table 1 (*Continued*)

Parameters	Total (*N* = 388)	Low eSBV/70 kg (*N* = 195)	High eSBV/70 kg (*N* = 193)	p value
PPP (%)	37 ± 8	37 ± 9	36 ± 8	0.623
LV E_{es}	2.00 ± 1.17	2.12 ± 1.26	1.88 ± 1.07	**0.021**
Alpha-LV	0.040 ± 0.017	0.040 ± 0.016	0.042 ± 0.019	0.353

ACE = angiotensin-converting enzyme; AL-CA = light-chain-cardiac amyloidosis; API = aorta pulsatility index; ARB = angiotensin-receptor blockers; BMI = body mass index; BP = blood pressure; CAD = coronary artery disease; CCB = calcium channel blocker; CI = cardiac index; CO = cardiac output; cTnI = cardiac troponin I; DPG = diastolic pulmonary gradient; Ees = end-systolic elastance; eSBV = estimated stressed blood volume; eTBV = estimated total blood volume; eUBV = estimated unstressed blood volume; GLS = global longitudinal strain; HF = heart rate; ICD = implantable cardioverter defibrillator; LAVi = left atrial volume index; LV = left ventricle; LVCPO = left ventricle cardiac power output; LVEDV = left ventricular end-diastolic volume; LVEF = left ventricular ejection fraction; LVESV = left ventricular end-systolic volume; mPAP = mean pulmonary artery pressure; MRA = mineralocorticoid receptor antagonist; NYHA = New York Heart Association; PAC = pulmonary arterial capacitance; PADP = pulmonary artery diastolic pressure; PASP = pulmonary artery systolic pressure; PCWP = pulmonary capillary wedge pressure; PP = pulse pressure; PPP = proportional pulse pressure; PVR = pulmonary vascular resistance; RAP = right atrial pressure; RVCPO = right ventricle cardiac power output; SAC = systemic arterial capacitance; SVR = systemic vascular resistance; TPG = transpulmonary pressure gradient.
Statistically significant values are highlighted in bold.

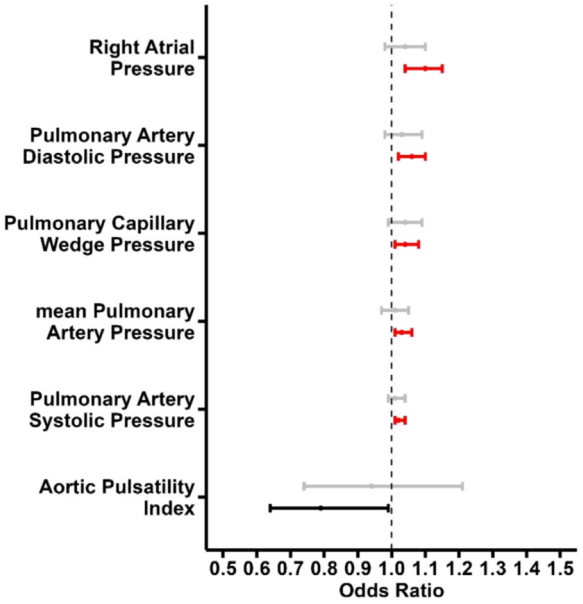

Figure 2. Forest plot displaying significant predictors of high estimated stressed blood volume in CA patients for Strata LVEF > 40% and LVEF ≤ 40%. Only LVEF > 40% is statistically significant. LVEF ≤ 40% bars are shown in gray.

proBNP, elevated eSBV emerged as an independent predictor for all-cause mortality (HR 2.19, 95% CI 1.19 to 4.03, p = 0.012) in this particular cohort (Table 2). Through the individual hemodynamic models for PCWP, CO, RAP/PCWP ratio, and PVR, elevated eSBV acts as an independent predictor for all-cause mortality. Yet, this risk was countered after adjustment for RAP (Table 2).

Determining eSBV and RAP interdependence in the LVEF > 40% cohort

To further elaborate the impact of RAP on SBV estimations and its relation to outcome, quartiles of high/low eSBV and high/low RAP were developed. Cut-offs for eSBV and RAP were based on the median 2,138 ml/70 kg and 12 mm Hg, respectively. Particularly, low eSBV/low RAP (*n* = 86), high eSBV/low RAP (*n* = 58), low eSBV/high RAP (*n* = 31), and high eSBV/high RAP (*n* = 58) were compared to determine their impact on clinical outcome. Figure 4 shows the unadjusted Kaplan–Meier curves of these quartiles for the primary endpoint of all-cause mortality in the LVEF > 40% cohort. Consistent to prior findings, there is limited impact of RAP on SBV estimations, suggesting that even when RAP is low, elevated eSBV might be (at least) equally harmful in CA patients with LVEF > 40% (Log-rank p = 0.008).

Discussion

Several notable findings emerged related to the role of eSBV as a detrimental hemodynamic feature in patients with CA (Graphical

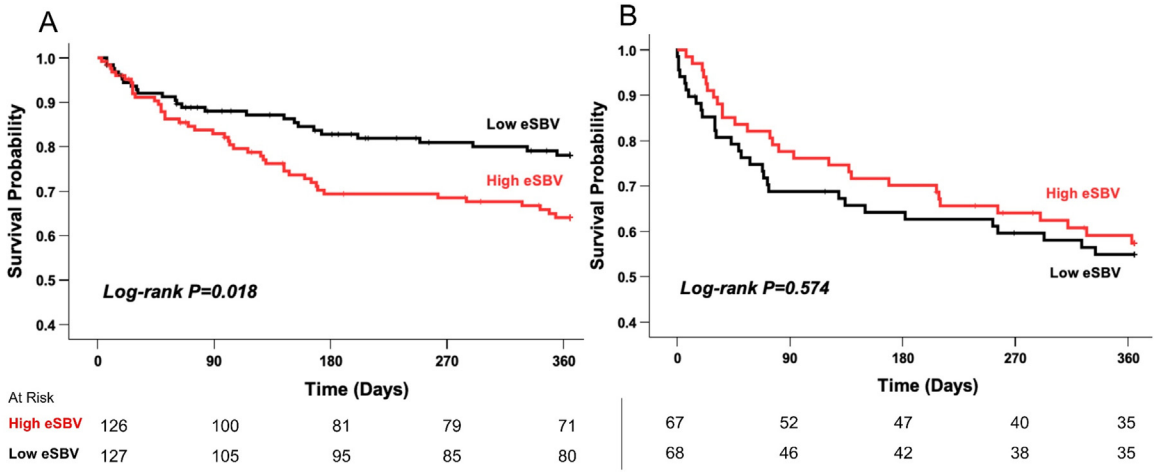

Figure 3. Kaplan–Meier estimates of low versus high estimated stressed blood volume in patients with heart failure stratified by LVEF > 40% (A) and LVEF ≤ 40% (B).

Table 2
All-cause mortality endpoint on univariate and multivariable Cox regression in LVEF > 40% adjusted for traditional cardiovascular risk factors and established hemodynamic parameters in het cohort

Model	Hazard ratio (95% CI)	p value
Univariable model	1.84 (1.12–3.01)	**0.015**
Multivariable model		
*Traditional CV risk factors**	2.19 (1.19–4.03)	**0.012**
Hemodynamic measurements		
RAP model	1.55 (0.91–2.64)	0.108
PCWP model	1.04 (1.00–1.07)	**0.026**
CO model	1.90 (1.12–3.22)	**0.017**
RAP/PCWP ratio model	1.81 (1.08–3.01)	**0.023**
PVR model	2.01 (1.11–3.62)	**0.021**

Significant p values are indicated in bold.
CO = cardiac output; CV = cardiovascular; PCWP = pulmonary capillary wedge pressure; PVR = pulmonary vascular resistance; RAP = right atrial pressure.
* Adjusted for age, sex, BMI, smoking history, ejection fraction, NT-proBNP.

Abstract). First, increased cardiac filling pressures and eSBV relative to TBV are observed in the majority of patients with CA. Second, the high eSBV mainly results in right-sided congestion (ie, increased RAP), yet acts as an independent hemodynamic feature in patients with LVEF > 40%. Third, in multivariable models, elevated eSBV is associated with an increased risk of all-cause mortality even after adjustment for traditional cardiovascular risk factors in patients with LVEF > 40%.

Patients with CA show biventricular amyloid accumulation which results in biventricular wall thinking and reduction in LV and RV cavity size.[16] This results in an upward and leftward shift in the LV end-diastolic pressure volume curve without compensatory changes of the end-systolic pressure volume relationship.[17–19] Concomitantly, the reduced stroke volume decreases cardiac output both at rest and during exercise hampering myocardial reserve and peak oxygen consumption.[20] These hemodynamically constrained ventricles tend to be highly sensitive to preload alternations. Meaning, any preload reduction (either by applying diuretics or venodilators) may underlie the narrow operational window in which eSBV preserves sufficient vascular (and ventricular) wall tension. Indeed, in contrast to the established inflammatory or obesity-associated HF with preserved LVEF phenotypes, patients with CA exhibit true diastolic HF, often presenting with diuretic or antihypertensive treatment intolerance. Although different hemodynamic profiles across amyloid phenotypes have been described previously, the largest cohort described by Martens et al comparing hemodynamic metrics in AL-CA and ATTR-CA found that AL-CA patients demonstrated higher PCWP (not RAP) and lower SVi, despite both groups having similar CI.[4–22] The investigators noted that AL-CA patients featured higher baseline heart rate, which corrected for their impaired SVi in maintaining CI, potentially linking AL-CA to a higher degree of diastolic dysfunction. However, in our total cohort, median eSBV was not significantly different between AL-CA and ATTR-CA patients.

Moreover, patients with CA are more likely to exhibit RV hypertrophy, causing a discordant rise in right-sided filling pressures and right ventricular-pulmonary artery uncoupling.[23] CA patients feature impaired ventricular filling (reduced LV end-diastolic volume) along with increased effective arterial elastance (Ea).[24] Mechanistically, CA patients with LVEF > 40% and higher eSBV likely have worse diastolic dysfunction, which drives fluid retention to maintain normal cardiac output and blood pressure. Additionally, our study results show that eSBV in CA patients with LVEF ≤ 40% is less predictive and correlates poorly with outcomes, potentially because the degree of diastolic dysfunction as a predominant driver of adverse outcomes in this cohort may be confounded by other variables of advanced disease. Intrinsically, hemodynamic profiles of patients featuring LVEF > 40% and LVEF ≤ 40% are highly distinctive, so direct comparison of both groups fell beyond the scope of this analysis.

Venous capacitance drives the relative portion of TBV that resides (functionally) in the stressed blood volume pool and therefore is a major determinant of cardiac filling pressures. Yet, how well venous capacitance may be impacted by chronic amyloid deposition in the splanchnic (and pulmonary) vasculature, especially in AL-CA, is unknown. Irrespective of the common autonomic nerve dysfunction seen in patients with CA, one potential consequence of chronic amyloid deposition on the splanchnic vascular bed is its ability to make it less compliant, which automatically leads to increases in stressed

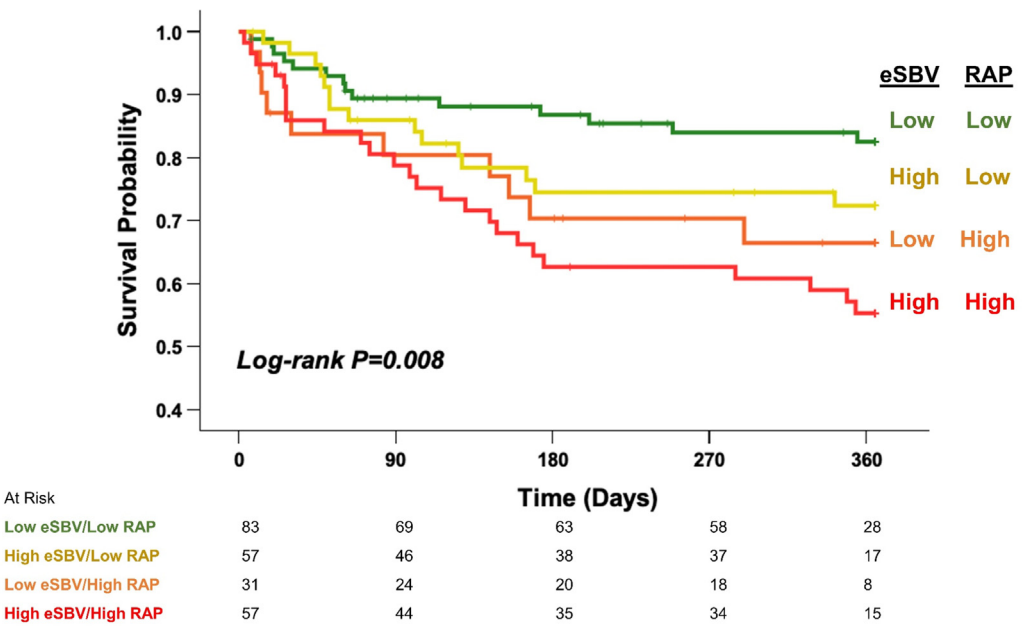

Figure 4. Kaplan–Meier estimates of quartiles high/low SBV and high/low RAP high in patients with LVEF > 40%.

blood volume.[25] The majority of our cohort showed elevated filling pressures at rest, yet predominantly displaying right-sided congestion. As shown in Figure 4, elevated eSBV in patients with LVEF > 40% appears to decouple from traditional RAP in terms of clinical outcomes, meaning that even in the context of low RAP, eSBV is (at least) equally harmful in clinical practice, and seems to be more reflective of pressure overload rather than volume overload. Although speculative, eSBV might be more sensitive in signaling (sub)clinical pressure overload in early-stage CA and therefore better predict the risk of future end-organ derangements. Also, a strong early hemodynamic clue of elevated stressed blood volume in clinical practice may therefore be reflected in a higher RAP/PCWP ratio, particularly in patients with LVEF > 40%. Indeed, LV end-diastolic pressure equals the sum of LV transmural wall tension and the external pressure applied by the pericardium or RV. To maintain RV preload, right cavity filling may cause septal shift while enhancing ventricular interdependence in patients with CA. This may further impede stroke volume and end-organ oxygenation, which potentially reflect worse clinical outcome in these patients.[20]

In general, invasive hemodynamic profiling of amyloid patients likely has the potential to detect intravascular pressure alternations and a sliding diastolic dysfunction early on in the disease trajectory, long before advanced signs and symptoms and/or echocardiographic derangements become apparent. Emerging disease-modifying amyloid treatments (eg, small-interfering RNAs, antisense oligonucleotides, gene editors, TTR stabilizers, TTR monoclonal antibodies) are particularly impactful in this early stage, yet hold a substantial healthcare-related cost burden. Traditional (serial) invasive hemodynamic profiling at an experienced, tertiary amyloid center might become essential to guide initial patient selection and the evaluation of treatment success. Consequential concomitant SBV estimations, which integrates features of these established invasive metrics, might increase the diagnostic power of the invasive study and guide to refer (or deter) a patient for potential disease-modifying treatments.

Study limitations

Several limitations should be highlighted. First, as this is a retrospective study, we cannot assess causality of eSBV to various hemodynamic phenotypes in CA throughout the LVEF spectrum. Second, since this is single-center study from a large tertiary referral center, selection and referral bias is likely, with those that are more symptomatic or with disease progression would have undergone hemodynamic assessments, while others who were too frail or aged may not have elected further invasive assessments. Third, all hemodynamic results only illustrate a snapshot of the hemodynamic profile at that time; accordingly, patients in both groups potentially received different HF treatments and be studied at different stages of disease. Additionally, the lack of data on specific genetic variant carriership may have limited our ability to assess its influence on eSBV and clinical outcomes in hereditary versus wild-type ATTR. Additional hemodynamic studies throughout different CA stages, more specifically displaying the degree of (extra)cardiac amyloid deposition, are warranted in order to better delineate distinctive phenotypes. Fourth, it would have been particularly interesting to capture responses in eSBV at rest and during exercise and responses to vasodilator testing, and whether these alternations impact clinical outcomes.[14,20] Fifth, to our understanding, there are currently no published data comparing algorithm-derived eSBV with “gold standard” serial measurements of mean circulatory pressure, hampering the generalizability of our study results. Additionally, we did not externally validate eSBV against established biomarker-based prognostic staging systems, including the National Amyloidosis Centre and Mayo staging systems. Sixth, the formula-derived model, which we applied to estimate TBV, does not always provide accurate measurements compared with direct quantitative measures of plasma (and total blood) volume.

Conclusions

In CA patients with LVEF > 40%, eSBV correlates well with traditional right-sided hemodynamic parameters as well as PCWP at rest. Estimation of stressed blood volume in CA patients with LVEF > 40% is an independent predictor of all-cause mortality even after adjustment for traditional cardiovascular risk factors. There is limited impact of RAP on SBV estimations, suggesting that even when RAP is low, elevated eSBV might be harmful. While eSBV also emerged as a factor contributing to outcomes in CA patients with LVEF ≤ 40% after accounting for differences in RAP, it was not as impactful as in the group with LVEF > 40%, which had a higher overall mortality. The data suggested that these patients have a more advanced stage of disease and diastolic dysfunction. Overall, the implementation of eSBV may enhance hemodynamic profiling of patients with CA and guide prognostication and assessment of treatment responsiveness.

Declaration of competing interest

The authors declare the following financial interests/personal relationships which may be considered as potential competing interests: Andres Carmona-Rubio, MD, reports a relationship with Pfizer, Inc that includes consulting or advisory. Trejeeve Martyn reports a relationship with FIRE1 that includes consulting or advisory. Trejeeve Martyn reports a relationship with Prolaio that includes consulting or advisory. Trejeeve Martyn reports a relationship with Boehringer Ingelheim/Eli Lilly that includes consulting or advisory. Trejeeve Martyn reports a relationship with Novo Nordisk that includes consulting or advisory. Trejeeve Martyn reports a relationship with Cleveland Clinic/American Well Joint Venture that includes consulting or advisory. Trejeeve Martyn reports a relationship with Pfizer that includes consulting or advisory. Trejeeve Martyn reports a relationship Apricity Robotics that includes consulting or advisory. Trejeeve Martyn reports a relationship Kilele Health that includes consulting or advisory. Trejeeve Martyn reports financial support was provided by Ionis Therapeutics (grant support). Trejeeve Martyn reports financial support was provided by AstraZeneca (grant support). Trejeeve Martyn reports financial support was provided by Heart Failure Society of America (grant support). Dr. Hanna reports a relationship with Alnylam Pharmaceuticals that includes consulting or advisory. Dr. Hanna reports a relationship with Eidos that includes consulting or advisory. Dr. Hanna reports a relationship with Akcea Therapeutics that includes consulting or advisory. Dr. Hanna reports a relationship with ATTRALUS that includes consulting or advisory. Dr. Hanna reports a relationship with Pfizer Inc that includes consulting or advisory. The Amyloidosis Registry is supported by Dr. Hanna’s Term Chair for Amyloid Heart Disease. Dr. Burkhoff has received equity from Harvi Dynamics Inc. Wai Hong Wilson Tang, MD reports financial support was provided by National Institutes of Health (grant support). Wai Hong Wilson Tang, MD, reports a relationship with Cardiol Therapeutics Inc that includes consulting or advisory. Wai Hong Wilson Tang, MD, reports a relationship with Zehna Therapeutics that includes consulting or advisory. Wai Hong Wilson Tang, MD, reports a relationship with WhiteSwell, Inc that includes consulting or advisory. Wai Hong Wilson Tang, MD, reports a relationship with Cardia-Tec Biosciences that includes consulting or advisory. Wai Hong Wilson Tang, MD, reports a relationship with Alleviant Medical, Inc that includes consulting or advisory. Wai Hong Wilson Tang, MD, reports a relationship with Alexion Pharmaceuticals, Inc that includes consulting or advisory. Wai Hong Wilson Tang, MD, reports a relationship with Salubris Biotherapeutics, Inc that includes consulting or advisory. Wai Hong Wilson Tang, MD, reports a relationship with BioCardia, Inc that includes consulting or advisory. Wai Hong Wilson Tang, MD, reports a relationship with Tenax Therapeutics, Inc that includes consulting or advisory.

Wai Hong Wilson Tang, MD, reports a relationship with BridgeBio Pharma, Inc that includes consulting or advisory. Wai Hong Wilson Tang, MD, reports a relationship with Vasa Therapeutics, Inc that includes consulting or advisory. Wai Hong Wilson Tang, MD, reports a relationship with Springer Nature that includes funding grants (editor). Wai Hong Wilson Tang, MD, reports a relationship with Belvoir Media Group that includes funding grants (editor). Dr. Vanhentenrijk is supported by a grant from the Belgian American Educational Foundation and Pfizer Cardiac Transthyretin Amyloid Fellowship. All other authors have no relationships to disclose.

CRediT authorship contribution statement

Simon Vanhentenrijk: Writing – original draft, Formal analysis, Data curation, Conceptualization. **Silvio Nunes Augusto Jr:** Writing – review & editing, Formal analysis. **Pieter Martens:** Writing – review & editing, Formal analysis. **Lauren Ives:** Writing – review & editing, Data curation. **Sanjeeb Bhattacharya:** Writing – review & editing. **Andres Carmona-Rubio:** Writing – review & editing. **J. Emanuel Finet:** Writing – review & editing. **Miriam Jacob:** Writing – review & editing. **Trejeeve Martyn:** Writing – review & editing. **Jason Valent:** Writing – review & editing. **Mazen Hanna:** Writing – review & editing. **Daniel Burkhoff:** Writing – review & editing. **Wai Hong Wilson Tang:** Writing – review & editing.

Supplementary materials

Supplementary material associated with this article can be found in the online version at https://doi.org/10.1016/j.amjcard.2026.02.025.

References

1 Ruberg FL, Maurer MS. Cardiac amyloidosis due to transthyretin protein: a review. JAMA 2024;331(9):778–91.
2 Ruberg FL. Phenotype mapping in cardiac amyloidosis. J Am Coll Cardiol 2021;78(22):2193–5.
3 Forrester JS, Diamond G, Chatterjee K, Swan HJ. Medical therapy of acute myocardial infarction by application of hemodynamic subsets (first of two parts). N Engl J Med 1976;295(24):1356–62.
4 Martens P, Bhattacharya S, Longinow J, Ives L, Jacob M, Valent J, Hanna M, Tang WHW. Hemodynamic profiling and prognosis in cardiac amyloidosis. Circ Heart Fail 2023;16(3):e010078.
5 Rapezzi C, Merlini G, Quarta CC, Riva L, Longhi S, Leone O, Salvi F, Ciliberti P, Pastorelli F, Biagini E, Coccolo F, Cooke RM, Bacchi-Reggiani L, Sangiorgi D, Ferlini A, Cavo M, Zamagni E, Fonte ML, Palladini G, Salinaro F, Musca F, Obici L, Branzi A, Perlini S. Systemic cardiac amyloidoses: disease profiles and clinical courses of the 3 main types. Circulation 2009;120(13):1203–12.
6 Fudim M, Kaye DM, Borlaug BA, Shah SJ, Rich S, Kapur NK, Costanzo MR, Brener MI, Sunagawa K, Burkhoff D. Venous tone and stressed blood volume in heart failure: JACC review topic of the week. J Am Coll Cardiol 2022;79(18):1858–69.
7 Gillmore JD, Maurer MS, Falk RH, Merlini G, Damy T, Dispenzieri A, Wechalekar AD, Berk JL, Quarta CC, Grogan M, Lachmann HJ, Bokhari S, Castano A, Dorbala S, Johnson GB, Glaudemans AW, Rezk T, Fontana M, Palladini G, Milani P, Guidalotti PL, Flatman K, Lane T, Vonberg FW, Whelan CJ, Moon JC, Ruberg FL, Miller EJ, Hutt DF, Hazenberg BP, Rapezzi C, Hawkins PN. Nonbiopsy diagnosis of cardiac transthyretin amyloidosis. Circulation 2016;133(24):2404–12.
8 Doshi D, Burkhoff D. Cardiovascular simulation of heart failure pathophysiology and therapeutics. J Card Fail 2016;22(4):303–11.
9 Lau V, Sagawa K, Suga H. Instantaneous pressure-volume relationship of right atrium during isovolumic contraction in canine heart. Am J Physiol Heart Circ Physiol 1979;236(5):H672–9.
10 Doshi D, Burkhoff D. Cardiovascular simulation of heart failure pathophysiology and therapeutics. J Card Fail 2016;22(4):303–11.
11 Alexander Jr J, Sunagawa K, Chang N, Sagawa K. Instantaneous pressure-volume relation of the ejecting canine left atrium. Circ Res 1987;61(2):209–19.
12 Maughan WL, Shoukas AA, Sagawa K, Weisfeldt ML. Instantaneous pressure-volume relationship of the canine right ventricle. Circ Res 1979;44(3):309–15.
13 Suga H, Sagawa K. Instantaneous pressure-volume relationships and their ratio in the excised, supported canine left ventricle. Circ Res 1974;35(1):117–26.
14 Sorimachi H, Burkhoff D, Verbrugge FH, Omote K, Obokata M, Reddy YNV, Takahashi N, Sunagawa K, Borlaug BA. Obesity, venous capacitance, and venous compliance in heart failure with preserved ejection fraction. Eur J Heart Fail 2021;23(10):1648–58.
15 von Elm E, Altman DG, Egger M, Pocock SJ, Gøtzsche PC, Vandenbroucke JP. The Strengthening the Reporting of Observational Studies in Epidemiology (STROBE) statement: guidelines for reporting observational studies. Lancet 2007;370(9596):1453–7.
16 González-López E, Gallego-Delgado M, Guzzo-Merello G, de Haro-Del Moral FJ, Cobo-Marcos M, Robles C, Bornstein B, Salas C, Lara-Pezzi E, Alonso-Pulpon L, Garcia-Pavia P. Wild-type transthyretin amyloidosis as a cause of heart failure with preserved ejection fraction. Eur Heart J 2015;36(38):2585–94.
17 Rosenblum H, Burkhoff D, Maurer MS. Untangling the physiology of transthyretin cardiac amyloidosis by leveraging echocardiographically derived pressure–volume indices. Eur Heart J 2020;41(14):1448–50.
18 Batra J, Rosenblum H, Cappelli F, Zampieri M, Olivotto I, Griffin JM, Saith SE, Teruya S, De Los Santos J, Argiro A, Burkhoff D, Perfetto F, Maurer MS. Racial differences in Val122Ile-Associated transthyretin cardiac amyloidosis. J Card Fail 2022;28(6):950–9.
19 Rosenblum HR, Griffin JM, Minamisawa M, Prasad N, Vest J, White MT, Solomon SD, Burkhoff D, Maurer MS. Effect of patisiran on stroke volume in hereditary transthyretin-mediated amyloidosis: insights from pressure-volume analysis of the APOLLO study. Eur J Heart Fail 2023;25(5):727–36.
20 Clemmensen TS, Mølgaard H, Sörensen J, Eiskjaer H, Andersen NF, Mellemkjaer S, Andersen MJ, Tolbod LP, Harms HJ, Poulsen SH. Inotropic myocardial reserve deficiency is the predominant feature of exercise haemodynamics in cardiac amyloidosis. Eur J Heart Fail 2017;19(11):1457–65.
21 Russo C, Green P, Maurer M. The prognostic significance of central hemodynamics in patients with cardiac amyloidosis. Amyloid 2013;20(4):199–203.
22 Duca F, Snidat A, Binder C, Rettl R, Dachs TM, Seirer B, Camuz-Ligios L, Dusik F, Capelle CDJ, Hong Q, Agis H, Kain R, Mascherbauer J, Hengstenberg C, Badr Eslam R, Bonderman D. Hemodynamic profiles and their prognostic relevance in cardiac amyloidosis. J Clin Med 2020;9(4):1093.
23 Maurer MS, Packer M. Impaired systemic venous capacitance: the neglected mechanism in patients with heart failure and a preserved ejection fraction? Eur J Heart Fail 2020;22(2):173–6.
24 Bhuiyan T, Helmke S, Patel AR, Ruberg FL, Packman J, Cheung K, Grogan D, Maurer MS. Pressure-volume relationships in patients with transthyretin (ATTR) cardiac amyloidosis secondary to V122I mutations and wild-type transthyretin: Transthyretin Cardiac Amyloid Study (TRACS). Circ Heart Fail 2011;4(2):121–8.
25 Kittleson MM, Maurer MS, Ambardekar AV, Bullock-Palmer RP, Chang PP, Eisen HJ, Nair AP, Nativi-Nicolau J, Ruberg FL. American Heart Association Heart Failure and Transplantation Committee of the Council on Clinical Cardiology. Cardiac amyloidosis: evolving diagnosis and management: a scientific statement from the american heart association. Circulation 2020;142(1):e7–e22.